Biochimica et Biophysica Acta, 1102 (1992) 91–106

BBABIO 43681

Electric field effect on the picosecond fluorescence of Photosystem II and its relation to the energetics and kinetics of primary charge separation

Holger Dau and Kenneth Sauer

Chemical Biodynamics Division, Lawrence Berkeley Laboratory and Department of Chemistry, University of California, Berkeley, CA (USA)

(Received 9 December 1992)
(Revised manuscript received 26 March 1992)

Key words: Charge separation; Diffusion potential; Fluorescence; Free energy; Picosecond; Thylakoid membrane; Time-resolved spectroscopy

Across the thylakoid membrane of spinach chloroplasts a diffusion potential of defined magnitude can be created by rapid changes in the KCl concentration. The resulting electric field leads to an increase in the yield of photosystem II (PS II) fluorescence for positive membrane voltages – positive in the inner thylakoid space – and a decrease for negative membrane voltages (Dau and Sauer, 1991, BBA 1098, 49–60). We have now studied this phenomenon by measurement of picosecond fluorescence decay. Based on the kinetic PS II model of Schatz et al. (1988, Biophys. J. 54, 397–405), the fluorescence decays were interpreted in terms of the rate constants of primary charge separation (formation of reaction center cation radical and pheophytin anion radical), primary charge recombination (recombination of primary biradical to chlorophyll singlet state) and secondary charge separation (reduction of primary quinone acceptor). For increasingly positive thylakoid voltages, the results are indicative of a relatively small but significant decrease in the rate constant of primary charge separation (by about 8% per +100 mV thylakoid voltage) and a much larger increase (by about 50% per +100 mV) of the rate constant of primary charge recombination. Nevertheless, due to the high sensitivity of the PS II fluorescence yield to changes in the rate constant of primary charge separation, the field-induced increase of fluorescence yield results mainly from the decreased rate constant of primary charge separation, and to a smaller extent (about one third of the increase) from the increased rate constant of charge recombination. The free energy difference of the primary radical pair was found to change by 17 meV per 100 mV thylakoid voltage. The relation between the rate constant of primary charge separation and the free energy difference appears to be linear within the accessible range of free energy changes (−15 meV to +22 meV); the rate constant of primary charge separation increases with increasingly negative free energy differences by 6% per 10 meV. This free energy dependence is compared with model calculations for a sequential two-step and for a super-exchange model of the primary PS II charge separation.

Introduction

In Photosystem II (PS II), a pigment/protein complex embedded in the thylakoid membrane of higher plants, light is absorbed by about 200 antenna pigments. The excitation energy is transferred rapidly to the reaction center, called P680, which is often assumed to be a dimer of chlorophylls (but see also Ref. 1). Following excitation of P680 an ultrafast (about 3 ps at 277 K [2]) charge separation reaction is initiated, which results in the formation of a chlorophyll cation radical ($P680^+$) and a pheophytin anion radical ($Pheo^-$). This primary charge separation may be followed by a secondary charge separation resulting in the reduction of a quinone (Q_a), by formation of triplet states or by recombination and reformation of the excited singlet state of the donor. The primary charge separation reaction competes with back transfer of excitation energy to the antenna and the consequent fluorescence. Membrane potentials and the resulting electric fields seem to affect the charge separation and/or recombination reactions, and thereby the so-called 'prompt' fluorescence emission of PS II [3–8].

Correspondence to: H. Dau, Chemical Biodynamics Division, Lawrence Berkeley Laboratory, 1 Cyclotron Road, Berkeley, CA 94720, USA.

Abbreviations: F_0, fluorescence with oxidized Q_a; F_m, fluorescence with reduced Q_a; ΔG, free energy difference; Pheo, primary acceptor pheophytin of PS II; P680, reaction center chlorophyll of PS II; PS, photosystem; Q_a, primary quinone acceptor of PS II; V, thylakoid voltage.

It has been proposed that electric fields, which result from an electric potential difference between inner and outer thylakoid space, may be of physiological importance for the control of PS II electron transfer [7,9,10]. Schatz et al. [11] put forward the hypothesis that local electric fields may be responsible for the fluorescence increase observed upon Q_a reduction, the so-called variable fluorescence. Furthermore, the controlled application of electric fields can facilitate the analysis of the free energy dependence of charge-separation reactions, which may serve as a criterion to elucidate the validity of different models of these reactions [12–16].

Recently we described a method to create membrane voltages of defined magnitude and polarity in thylakoid preparations of spinach by means of a salt-jump technique [8]. It was found that in the open reaction center state, i.e., with oxidized Q_a, the PS II fluorescence yield increases with positive thylakoid voltages (positive at the inner thylakoid side) and decreases with negative thylakoid voltages. We concluded from the analysis of emission spectra and the trap-closure sensitivity that this electric field effect on the fluorescence emission arises from an influence on the PS II charge separation reactions. However, the observed electric field effect on the fluorescence emission may arise from an effect on the primary charge separation, primary charge recombination or even from an effect on the secondary charge separation (see Eqn. A7 and A10 in the Appendix). The analysis of the steady-state fluorescence emission cannot determine which charge transfer reaction effects result in the electric field effect on the fluorescence emission or how the rate constants, which describe the different PS II charge separation reactions, change in response to the electric field. To address these questions, we have investigated the effect of electric fields on the picosecond kinetics of the PS II fluorescence.

To relate the picosecond fluorescence kinetics of PS II to the charge separation reactions, it is necessary to use a specific kinetic model. Our analysis of the electric field effect on the PS II charge-separation reactions is based on the so called 'reversible radical pair model' [9,11,17] for the room temperature fluorescence emission of higher plant PS II's, which is outlined in the Appendix. This model has been confirmed by picosecond studies on the fluorescence emission [9,18–20], absorbance changes [11,18] and photoelectric signals [9]. Arguments in favor of this model have recently been reviewed by Holzwarth [21]. We find that the reversible radical pair model facilitates the determination of the thylakoid voltage dependence of individual rate constants of PS II charge separation. In particular, for a certain range of free energy differences, we obtain the free energy dependence of the rate constant of primary charge separation.

The primary PS II charge separation proceeds with a time-constant of about 3 ps at 277 K [2] and of about 1.5 ps at 15 K [22]. It can be concluded from sequence homologies with bacterial reaction center proteins [23] that the distance between the donor chlorophyll(s) and the pheophytin is similar to the respective distance in the bacterial reaction center, i.e., about 1 nm edge-to-edge distance of the chromophores. Theoretical considerations [24] and experiments on different inner-protein electron transfer reactions [25,26], however, predict for a 1 nm electron transfer a charge separation rate which is slower than the experimentally determined values by about two orders of magnitude. Thus in analogy to the situation in photosynthetic bacteria, a still unknown or undetermined mechanism or interaction seems to facilitate these ultrafast long-distance electron transfers. One way of addressing this question is from the analysis of the free-energy dependence of the charge separation reaction as provided by electric field studies. The free-energy dependence of charge separation reactions is assumed to be distinctively different for different electron transfer mechanisms [12,13,26]. In the Discussion, the experimentally determined free-energy dependence of the rate constant of primary PS II charge separation is compared with relations predicted by different theories of primary charge separation.

Materials and Methods

Creation of diffusion potentials across thylakoid membranes

Thylakoid membranes were prepared from spinach as described in Ref. 8.

All solutions used in the experiments contained 2 mM $MgCl_2$ and 2 mM Hepes, adjusted to pH 7.1 with NaOH. The KCl concentrations were chosen as specified in the text. To obtain always the same osmotic strength of the medium [8], the sorbitol molar concentration was determined according to: $[\text{sorbitol}] = 330\ \text{mM} - 2 \cdot [\text{KCl}]$.

To create a diffusion potential across the thylakoid membranes, the inner thylakoid space was 'pre-loaded' with a KCl concentration $[\text{KCl}]_0$ and then various outer-thylakoid salt concentrations, $[\text{KCl}]^{out}$, were established by means of the flow and mixing technique described below.

10 min before starting the experiment, the thylakoid membranes, and 2 μM of the potassium-specific ionophore valinomycin, were suspended in a solution with the KCl concentration $[\text{KCl}]_0 = 27$ mM, except in the case of data points in Figs. 6 and 7 marked by a square, where it was 0.65 mM.

During the measurements the dark-adapted thylakoid-containing solution was continuously mixed with solutions of different KCl content as follows. The two

solutions were pumped by two peristaltic pump heads synchronously driven by one motor drive (Cole and Parmer, Masterflex drive 7520-25). After mixing the two solutions by means of a T-type tube-connector, the solutions flowed through a tube of 7 cm length to ensure complete mixing. Then the picosecond fluorescence measurements were made using a fluorimeter flow-cell of square cross-section (2 × 2 mm). Based on the flow-rate and the dimensions of tubing and measuring cell, it was calculated that the measurements were made within 200 ms after mixing the two solutions. The ratio of the flow rate of the salt solution to the flow rate of the thylakoid solution was usually 13. The ratio was 1 in the case of data points in Figs. 6 and 7 marked by a square. The chlorophyll content after mixing was between 20 and 40 μg/ml.

The thylakoid voltage after mixing was calculated from the KCl concentration of the initial thylakoid solution, $[KCl]_0$, and the KCl concentration of the medium resulting from the mixing process, $[KCl]^{out}$, according to

$$V = 59\ mV \cdot \log([KCl]^{out}/[KCl]_0) \quad (1)$$

For further details on this salt-jump technique see Ref. 8.

Picosecond fluorescence measurements

Fluorescence measurements were made at room temperature (25–28°C) by time-correlated single-photon counting.

The fluorescence excitation source was a Spectra Physics synchronously pumped mode-locked dye laser (argon ion laser Model 2040, dye laser Model 375, cavity dumper Model 344). Thylakoids in the flow cell described above were excited at 616 nm and at 4 MHz repetition rate.

Fluorescence photons were detected at 683 ± 5 nm by a microchannel-plate photomultiplier (Hamamatsu R2809U). The single-photon timing system and the numerical analysis have been described previously [27]. The channel width was 10 ps/channel. All decays were measured with 10000 counts in the peak channel. The instrument response function was determined at the excitation wavelength using a light-scattering suspension; the half-maximum full-width duration was 80–90 ps.

Due to low-intensity laser pulses (50 W m^{-2}) and an exposure time of the dark-adapted thylakoids to the laser beam of less than 3 ms, all measurements were done in the open reaction-center state of Photosystem II (F_0-state). The data shown in Fig. 3 stem from six fluorescence decays all measured using the same reservoir of thylakoid-containing solution. The six decays were measured within 35 min (about 4 min measuring time, t_d, per decay); the sequence of KCl concentrations was random and not monotonically increasing or decreasing.

By curve-fitting, employing iterative deconvolution with the instrument response function, all fluorescence decay data were resolved into a sum of exponentials described by the pre-exponential factor A_i (in the following called 'amplitudes') and the time-constants T_i. As usual, an additional free parameter of these fits was the co-called 'shift' between the instrument response function and the fluorescence decay. (This parameter accounts for the possibility that there is a shift between the time-axis, i.e., channel number, of the fluorescence decay and the time-axis of the instrument response function, which was determined before starting the fluorescence experiment by using a scatter solution [27]. Such a shift may arise from instability or drift in the properties of the electronics which provides the start and the stop pulse for the time-to-voltage converter.) The determined shift parameters did not exhibit any obvious correlation with the applied thylakoid voltage. The quality of a fit was judged both from a plot of the weighted residuals and by the value of the reduced χ^2 value. Visual inspection of the plot of the weighted residuals never revealed any deviations which appeared to be non-random. Reduced χ^2 values of the fits were always between 1.0 and 1.15. The plots of the weighted residuals and the χ^2 values indicate that the deviations between the data and the mathematical representation of the data by a sum of three exponentials is due only to the inevitable statistical noise of the single-photon counting technique.

The following parameters and functions were calculated from the amplitudes, A_i, the time-constants, T_i, and the measuring time for each experiment, t_d:

relative amplitudes	$a_i = A_i / (\sum A_i)$	(2)
amplitude	$A = (\sum A_i) \cdot t_d$	(3)
initial slope	$S_0 = \sum a_i / T_i$	(4)
mean lifetime	$T_m = \sum a_i \cdot T_i$	(5)
second moment	$M = \sum a_i \cdot T_i^2$	(6)
deconvoluted decay	$F(t) = \sum a_i \cdot e^{-t/T_i}$	(7)
difference decay	$\Delta F(t) = F'(t) - F(t)$	(8)

Error ranges and error propagation

The straight lines in the Figs. 3C, 5, 6, 7 were determined by a least-squares fit to the data points. The slope values and the zero-field values given in the text and in Table I result from these fits to a straight line (linear regression); error ranges given for the slope values and the zero-field values are the standard errors of the estimated values.

The error bars displayed in the Figs. 5–7 were determined as follows: S_0, T_m and M were calculated from the data set shown in Fig. 3. The plots of these parameters vs. the thylakoid voltage were fitted by straight lines (linear regression), the standard errors of the slope values and the zero-field values (given in the Results section) were relatively low. Therefore, we used the standard deviation from the straight line (ΔS_0, ΔT_m and ΔM, respectively) as an estimate of the respective error. The errors of these three parameters were assumed to be independent; the errors of the rate constants and of the change in free energy were calculated according to ($y = k_1$, k_{-1}, k_2 and $\Delta\Delta G$, respectively)

$$\Delta y = \mathrm{SQRT}\{\{(\partial y/\partial S_0)\Delta S_0\}^2 + \{(\partial y/\partial T_m)\,\Delta T_m\}^2 + \{(\partial y/\partial M)\,\Delta M\}^2\}$$

with the values of the partial derivatives taken at the zero field values of S_0, T_m and M. The error bars given in the Figs. 5–7 indicate the range given by $y \pm \Delta y$.

Results

Thylakoid membranes suspended in a 27 mM KCl medium were continuously mixed with a medium of the same or a different KCl content as described in Materials and Methods. The resulting thylakoid voltage is given by Eqn. 1 [8]. We have analyzed the influence of these salt-induced thylakoid voltages on the pulse-induced relaxation kinetics of the chlorophyll fluorescence within a time window of 9.5 ns after the laser flash (for details see Materials and Methods).

Fig. 1 shows the fluorescence decays measured without thylakoid voltage (lower curve) and with a positive thylakoid of 46 mV (upper curve). Already upon application of this relatively low thylakoid voltage, an electric-field-induced difference in the fluorescence-relaxation kinetics is detectable by a visual inspection of the decay plots (see inset of Fig. 1). However, mainly due to high-frequency noise components, the difference is obscured by noise.

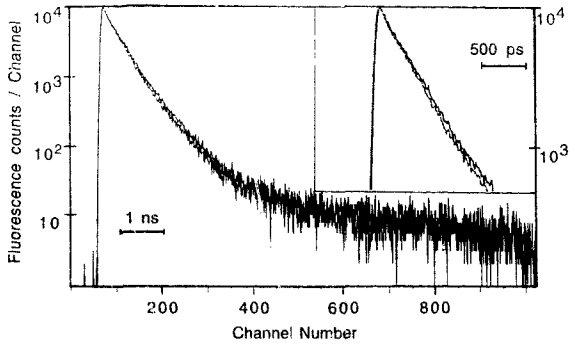

Fig. 1. Fluorescence decay with a salt-induced thylakoid voltage of +45 mV (lower line) and the zero-voltage decay (upper line). The curve-fitting results for both decays are given in Fig. 3.

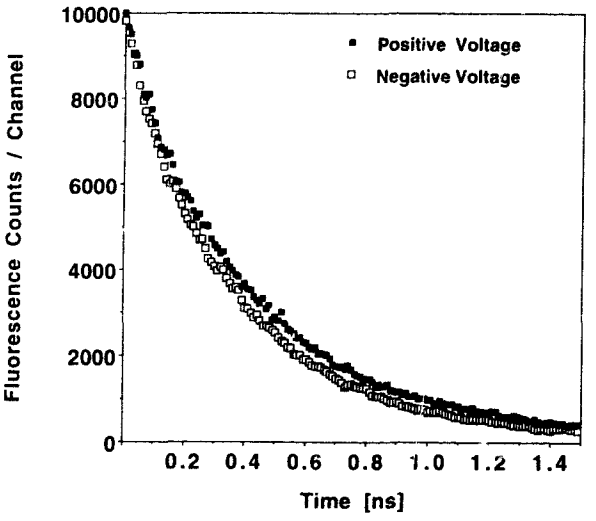

Fig. 2. Fluorescence decays with +45 mV and −69 mV thylakoid voltage. The fluorescence counts per channel are given for all channels which cover a time-range of 1.5 ns after the peak-channel. The curve-fitting results for both decays are given in Fig. 3.

In Fig. 2 the decays obtained upon application of a positive thylakoid voltage (+46 mV) and a negative thylakoid voltage (−69 mV) are shown. The zero-field decay curve, which is not shown, lies between the two curves. Already these 'raw data' demonstrate that the initial slope of the decay (slope of a straight line through the first five data points, corresponding to the first 50 ps) is changed upon application of the electric field; the difference between the decay curves is maximal between 300 and 600 ps after the peak of the decay and the absolute difference at 1.5 ns, though low, is not zero (about one third of maximum difference). However, the raw data decays shown in Fig. 2 are still the result of the convolution of the measuring system response-function and the biological system response-function, and the 'fast' noise is still of considerable magnitude. Therefore, the decays were subjected to curve-fitting and iterative deconvolution (as described in Materials and Methods) and the results were used for a more detailed analysis of the electric-field effect.

Curve-fitting of the measured fluorescence decays reveals that they are very well described by a sum of three exponentials. The resulting amplitudes and time-constants are shown in Fig. 3A and B for a typical set of fluorescence decays.

The slowest lifetime component contributes to the amplitude by only 0.2 to 0.4%. The time-constant and relative amplitude of this component show a slight

electric field dependence; however, the yield of this component ($=a_3 \cdot T_3$) remains almost constant (not shown). This long-lived component is assumed to originate from 'impurities', such as a small amount of closed PS II reaction centers and/or free chlorophylls [10,19,20,21,28]. We assume that the slight observed electric field dependence results from the incapability of the curve-fitting routines to resolve this component with sufficient accuracy in the presence of electric-field dependent lifetime components of 100-times greater relative amplitude. In the following, this lifetime component is not considered further. In the calculations of parameters from the amplitudes and time-constants described below the slow component was not included. (In any event, due to its small amplitude an inclusion of this component leads to almost the same results.)

Fig. 3C gives the amplitude and the mean life time calculated according to Eqns. 3 and 5, respectively, from the results of the exponential fit. Obviously, the electric field affects the mean life time and not the amplitude. Changes of rate constants for fluorescence decays should lead to changes in the amplitude (see

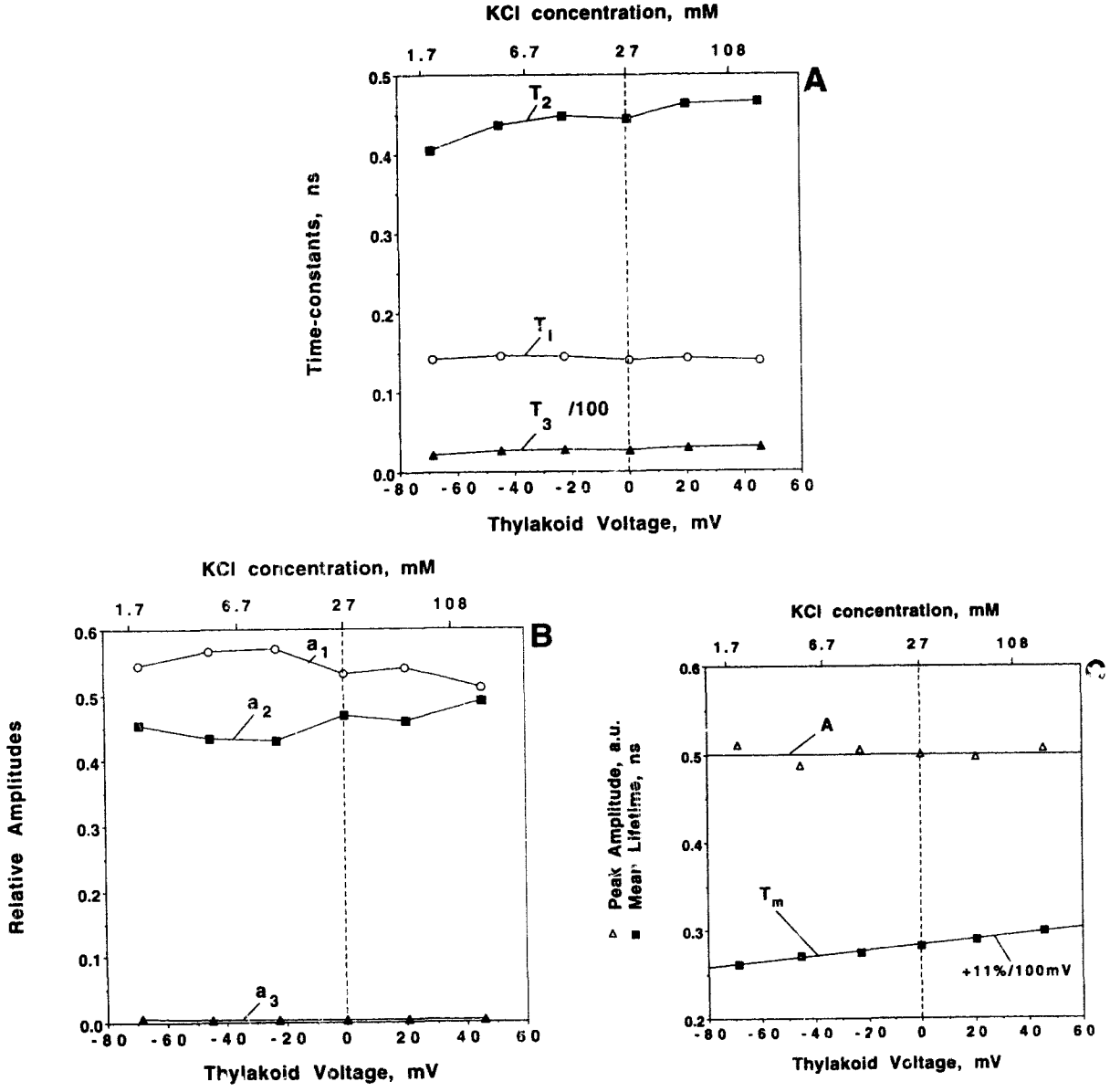

Fig. 3. Results of tri-exponential fits of fluorescence decays for different thylakoid voltages. The upper scales give the KCl concentration after mixing. The lower scales indicate the resulting thylakoid voltages calculated according to Eqn. 1. (A) Time-constants; (B) relative amplitude; (C) peak amplitude and mean lifetime. (In A, the time-constant value for T_3 has been divided by a factor of 100 to avoid inflation of the ordinate scale.)

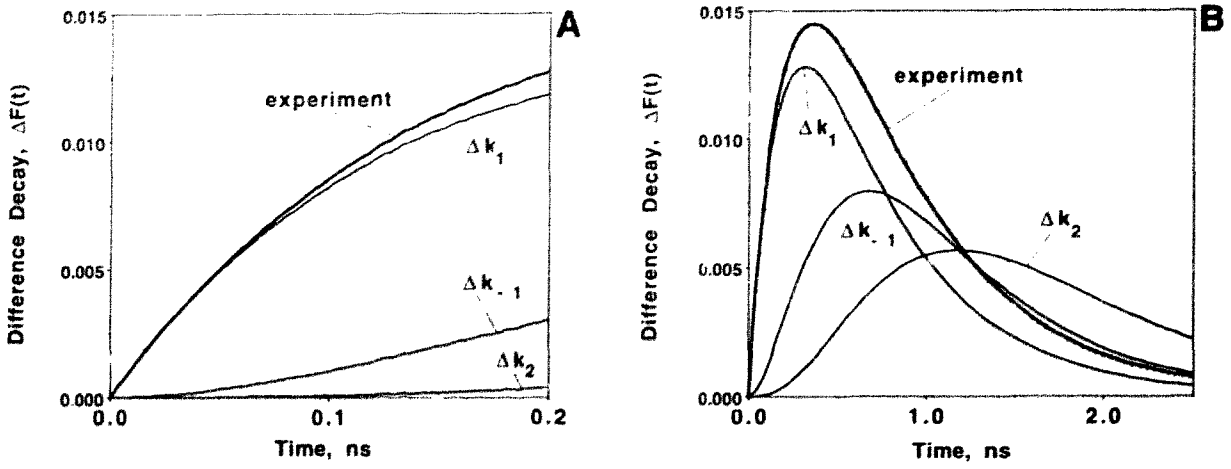

Fig. 4. Simulated and experimentally determined difference decays. The simulations are based on the reversible radial pair model with the following zero-field rate constants: $k_1 = 3$ ns^{-1}, $k_{-1} = 0.3$ ns^{-1}, $k_2 = 2.3$ ns^{-1} [20]. For each of the three solid lines only one rate constant has been varied to get a change in mean lifetime by 3.4% (variation of k_1 to 2.885 ns^{-1}, of k_{-1} to 0.393, of k_2 to 1.76 ns^{-1}). The experimental curve gives the difference between a decay with 46 mV thylakoid voltage and a decay with 0 mV thylakoid voltage, respectively, calculated according to Eqn. 8 from the data shown in Fig. 3. (A) Difference decays within 200 ps after delta-pulse excitation; (B) difference decays within 2.5 ns after excitation.

Appendix A, Eqns. A7, A8). Because the amplitude remains constant, our previous conclusion, that the electric field does not change the radiative decay rate constants, is confirmed. The mean lifetime, which was calculated according to Eqn. 5 from the amplitudes and time-constants of the three exponential components, increases linearly with the thylakoid voltage by $11 \pm 0.6\%$ per 100 mV thylakoid voltage. This compares very well with the previously observed increase of the steady state fluorescence emission at 680 nm [8].

In Ref. 8 the question was raised about which PS II charge-transfer reaction is responsible for the electric field effect on the fluorescence emission. To assess whether the time-resolved fluorescence data have the potential to answer this question, the changes in the fluorescence decays due to changes of individual charge-transfer rate constants were simulated, based on the reversible radical-pair model [11] using the rate constants determined by Roelofs et al. [20].

The experiment curve in Fig. 4 gives the difference between the 0 mV and the +46 mV fluorescence decay, as calculated from the data shown in Fig. 3 according to Eqn. 8. The difference decays calculated for other thylakoid voltages have essentially the same shape (not shown). Some essential features of these difference decays calculated from the curve-fitting results are also obvious from a closer inspection of the raw-data decay shown in Fig. 2: namely, the difference rises with a positive slope at $t = 0$, the maximum is reached at about 450 ps, the difference at 1.5 ns is about one fourth of the maximum difference. The other lines in Fig. 4 show simulated differences in the fluorescence decays resulting from changes of the rate constants of primary charge separation (k_1), primary charge recombination (k_{-1}) and secondary charge separation (k_2), respectively. For each of the three simulated difference decays, one rate constant was changed to get an increase in the mean lifetime by 3.4%, while the other rate constants remained unchanged. This was accomplished by a change of k_1 by 3.8%, of k_{-1} by 31%, and of k_2 by 23%. (The magnitude of the Δk_1 change of the simulation, which leads to a change in the mean lifetime by 3.4%, was chosen to get a fit of the initial slope of the experimental decay.)

The amplitudes ($t = 0$) of the simulated decays and the measured decays were set to be equal. This constitutes an approximation, because PS I contributes to the amplitudes of the measured decays. Consideration of a PS I contribution, which does not depend on the thylakoid voltage, would require only a re-scaling of the experimental difference decay, resulting in an increase of all ordinate values of the experimental difference decay by the same factor (10 to 30% increase, depending on the assumed contribution of PS I). The conclusions given below, however, are the same, regardless of whether the PS I contribution to the amplitude is considered (see also Discussion).

The simulation of the difference decays and the comparison with experimentally determined difference decays reveal:

(1) changes of individual rate constants influence the fluorescence decays in distinctive ways. Thus, anal-

ysis of time-resolved fluorescence data should help to elucidate the origin of the electric-field effect on the fluorescence emission;

(2) all three charge separation/recombination rate constants influence the fluorescence decays. However, to get a comparable effect on the mean lifetime, the relative changes of k_{-1} and k_2 have to be much greater than the changes of k_1. This means that, as predicted by Eqn. A10, relatively small changes of k_1 are more likely to be detectable than comparable changes of k_{-1} and k_2, which may be below the detection limit;

(3) already a visual comparison of the experiment curve in Fig. 4, with the simulated curves, indicates that the electric field effect on the PS II fluorescence emission results from a change of the rate constant of primary charge separation and most likely also of the rate constant of primary charge recombination. The origin of the electric field-induced change in the fluorescence yield seems to be not a change of the rate constant k_2 (though changes of k_2 cannot be ruled out, see Discussion). A nearly perfect fit (not shown) of the experimental curve is obtained, if k_1 is changed from 3 to 2.885 ns^{-1} and k_{-1} from 0.3 to 0.329 ns^{-1} if k_2 remains constant. Also the difference decays for other thylakoid voltages were calculated and compared to simulations (not shown). In each case the comparisons indicate that the electric field-induced increase/decrease in the PS II fluorescence yield arises mainly, but not exclusively, from a decrease/increase of the charge separation rate constant k_1; about one third of the electric field effect on the fluorescence yield seems to originate from increase/decrease of charge recombination rate constant k_{-1}.

Now we shall relate the amplitudes and time-constants shown in Fig. 3 directly to rate constants of the PS II charge separation reactions using the reversible radical pair model of PS II (see Appendix A). To do so the initial slope, S_0, of the decay, the mean lifetime, T_m, and the second moment, M, were calculated (Eqns. 4–6). All three parameters depend linearly on V, the thylakoid voltage: $S_0 = 4.83\{0.2\%\} - 2.0\{13\%\}\ V$; $T_m = 0.283\{0.2\%\} + 0.32\{5\%\}\ V$; $M = 0.130\{0.5\%\} + 0.33\{5\%\}\ V$; S_0 in ns^{-1}, T_m in ns, M in ns^2; the values in brackets give the standard errors of the estimates; the thylakoid voltage dependence of T_m and the fit by a straight line are shown in Fig. 3C, the S_0 and M curves are not shown. These parameters were corrected for the PS I contribution according to Eqn. B5. It was assumed that the PS I fluorescence can be represented by a single exponential, with an amplitude of 22% of the peak amplitude and a time-constant of 100 ps. Using the corrected parameters, the rate constants k_1, k_{-1}, k_2 and the change of the free energy difference, $\Delta\Delta G_1$, were determined according to Eqns. A11–A17 with a value of 0.3 ns^{-1} for k_A, the rate constant for radiative and nonradiative decays of excited antenna chlorophylls. The resulting rate constants are shown in Fig. 5.

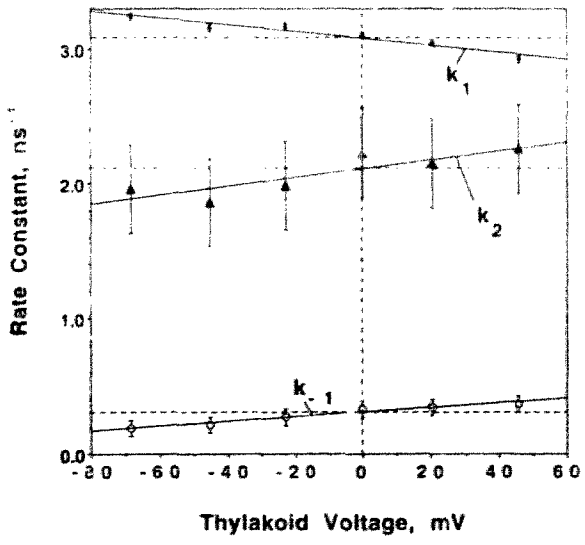

Fig. 5. Thylakoid-voltage dependence of the PS II rate constants for primary charge separation (k_1, closed squares), primary charge recombination (k_{-1}, open circles), and secondary charge separation (k_2, closed triangles).

The slope of the k_1 line in Fig. 5 indicates that the rate constant k_1 decreases by $8 \pm 1\%$ per 100 mV increase in thylakoid voltage; the rate constant k_{-1} increases by $56 \pm 6\%$ per 100 mV. Also the rate constant k_2 seems to increase by $15 \pm 6\%$ with increasing thylakoid voltages. However, taking into consideration the relatively small sensitivity of the fluorescence decay to changes of k_2, as discussed above, and the appreciable scatter of the k_2 values, we consider this increase to be of doubtful significance.

Using the results of Fig. 5, i.e., the k_1 and k_{-1} values, it becomes possible to calculate the shift in the free energy difference, $\Delta\Delta G_1$, which results from the salt-induced thylakoid voltage. In Fig. 6 the relation between changes in the free energy difference of the primary charge separation reaction and the thylakoid voltage is shown.

In the case of the data set discussed so far, the initial potassium chloride content of the thylakoid solution was $[KCl]_0 = 27$ mM. The choice of the $[KCl]_0$ determines the accessible range of positive thylakoid voltages [8]. To extend this range, experiments with $[KCl]_0 = 0.65$ mM were done; $\Delta\Delta G_1$ and k_1 were determined as described above. In Fig. 6 and Fig. 7, the resulting values are displayed, together with the values of the data set with $[KCl]_0 = 27$ mM.

It was a goal of this study to determine the free energy dependence of the primary charge separation reaction. Fig. 6 provides a calibration of the changes in

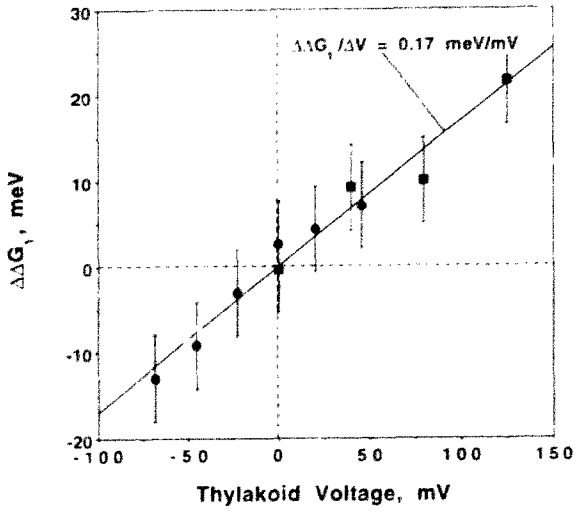

Fig. 6. Relation between thylakoid voltage, V, and the change in free energy difference of the primary charge separation reaction, $\Delta\Delta G_1$. The KCl concentration of the thylakoid solution before mixing was either 0.65 mM (closed squares) or 27 mM (closed circles); the thylakoid voltage is calculated according to Eqn. 1. The slope of the straight line is indicated in the figure.

free energy, $\Delta\Delta G_1$, which result from the salt-induced thylakoid voltage. The slope of the straight line in Fig. 6 indicates that the free energy difference of the primary charge separation reaction changes by 17 meV (± 1 meV) per 100 mV thylakoid voltage. Using this calibration factor, i.e. 0.17 meV/mV, the relative value (normalized to the zero-field value) of the rate constant of primary charge separation, as a function of the field-induced change in free energy difference, is plotted in Fig. 7. The relation between free energy shift and the rate constant of primary charge separation, k_1, appears to be linear; the rate constant increases for an increasingly negative free energy difference by about 6% ($\pm 0.5\%$) per 10 meV.

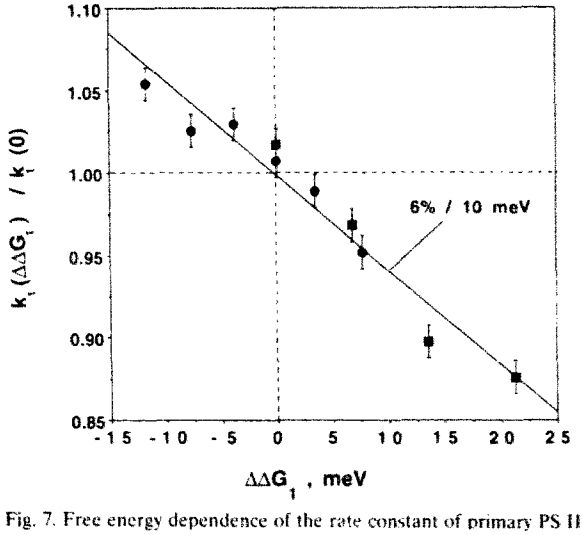

Fig. 7. Free energy dependence of the rate constant of primary PS II charge separation. The KCl concentration of the thylakoid solution before mixing was either 0.65 mM (closed squares) or 27 mM (closed circles); the thylakoid voltage is calculated according to Eqn. 1. The slope of the straight line is indicated in the figure.

Based on the PS II model of Schatz et al. [11], the rate constants k_1, k_{-1} and k_2 were determined from the experimental data, as described above. To do so, we corrected for the PS I contribution to the picosecond fluorescence kinetics, assuming a mono-exponential PS I decay with $T_{PSI} = 100$ ps, $a_{PSI} = 22\%$, and we used a value for the rate constant of antenna decay, $k_A = 0.3$ ns^{-1}. The parameters (T_{PSI}, a_{PSI}, k_A) were not experimentally determined. Although the assumed values are reasonable and in good agreement with other studies [20,28,29], the precise values are not known. To test the chosen values for the PS I correction, we also analyzed the zero-field decays of the fluorescence emission at 725 nm, which is enriched in contributions of PS I. Correction of the 683 nm decay and the 725 nm decay with $T_{PSI} = 102$ ps, $a_{PSI,683} = 0.225$ and $a_{PSI,725} = 0.57$ results in the same set of rate constant values. Such a consistent interpretation of the two decays measured at these two emission wavelengths was not obtainable for other values for T_{PSI} or a_{PSI}. However, if the time constants or amplitudes, which result from the tri-exponential fits of the measured decays, are varied slightly, a consistent interpretation of the decays measured at different wavelengths is obtained with clearly different values for T_{PSI} and a_{PSI}. We conclude that there remains an uncertainty about which values are most appropriate for the PS I correction.

To assess how sensitive the determined parameters are to the PS I correction and to the value of k_A, the

TABLE I

Parameter changes resulting from a variation of the assumed PS I time-constant, T_{PSI}, by 10% or the antenna decay rate constant, k_A, by 50%

The listed values were obtained by evaluating the data set shown in Fig. 3. The values stem from a least-squares fit of the parameter vs. thylakoid-voltage relation to a straight line. The rate constants and ΔG_1 give the resulting 0 mV value of this fit; the bottom three lines refer to the slopes.

T_{PSI} (ps)	100	110	100
k_A (ns^{-1})	0.3	0.3	0.15
k_1 (ns^{-1})	3.08	3.33	3.23
k_{-1} (ns^{-1})	0.31	0.66	0.29
k_2 (ns^{-1})	2.12	2.9	2.14
ΔG_1 (meV)	−182	−161	−179
$\Delta\Delta G_1$ (eV)/100 mV	18	12	18.6
Δk_1/100 mV (%)	−8.2	−7.5	−7.8
Δk_{-1}/100 mV (%)	+56	+44	+56

data shown in Fig. 5 were also evaluated with a 10% higher T_{PSI} and a 50% lower k_A, respectively. The results are summarized in Table 1.

It is obvious from Table 1 that the results do not depend critically on the value of k_A. However, some of the determined parameters are highly sensitive to the PS I correction. Especially, the value of the rate constant for primary charge recombination, k_{-1}, is extremely sensitive to T_{PSI}, indicating a considerable resulting uncertainty in the zero-field free energy difference of the primary charge separation reaction. Also, the important calibration factor given in the seventh line, which relates the thylakoid voltage to the shift of the free energy level of the primary radical pair, changes by about 30% from 18 to 12 eV/100 mV. By contrast, the rate constant of primary charge separation, k_1, and its relation to the thylakoid voltage are not especially sensitive to the PS I correction.

Discussion

Origin of the electric field effect on the fluorescence emission

The comparison of the fluorescence difference decays with simulations based on the kinetic PS II model of Schatz et al. [11] identifies which charge separation reactions are responsible for the electric field effect on the yield of PS II fluorescence: the previously observed electric field effect on the fluorescence yield, i.e., an increase of the yield by about 10% per 100 mV increase in thylakoid voltage [8], results mainly (about two thirds) from a decrease of the rate constant of primary charge separation and, to a smaller extent (about one third of the yield change), from an increase in the rate constant of primary charge recombination; the yield increase does not stem from an electric field effect on the secondary charge-separation reaction. (However, as discussed below, this secondary charge separation reaction may be affected to some extent, but this effect is too small to result in detectable fluorescence changes.) The simulations which lead to these conclusions rely on four premises:

(1) the validity of the PS II model of Schatz et al. [11] is assumed. This point has already been discussed in the Introduction. Furthermore, confidence in the validity of this model is strengthened by this study, because this model leads to a consistent interpretation of the electric field data (e.g., the linear relation between thylakoid voltage and free energy shown in Fig. 6);

(2) an appropriate set of rate constants for the zero-field decay [20] is assumed. This assumption is unproblematic, because variations of these rate constants within a reasonable range do not affect the conclusion that the electric field effect results mainly from an effect on the primary charge separation (about two thirds) and to a lesser extent (about one third) on the rate constant of secondary charge separation. However, the zero-field rate constants influence the magnitude of the relative changes of k_{-1} which have to be invoked to simulate the experimental decays (data not shown, but see also Table 1);

(3) it is assumed that the PS I fluorescence does not exhibit an electric field effect. This assumption is based on the spectral dependence of the electric field induced increase in the fluorescence emission and the sensitivity of this increase to DCMU [8]. (The prompt PS I fluorescence is only slightly or not at all determined by the charge separation reactions, as indicated by the absence of a variable PS I fluorescence [30]. Therefore, the insensitivity of the prompt PS I fluorescence to electric fields does not imply that the PS I charge separation reactions do not respond to electric fields);

(4) the rate constant for non-radiative decays is assumed to be not affected by electric fields. Gottfried et al. found that, in the isolated B800-850 antenna complex of photosynthetic bacteria, electric fields affect the non-radiative decays of excited antenna states [31]. However, the absence of any electric field effect on the fluorescence yield of PS II in the closed reaction center state (reduced quinone acceptor) [8] indicates that this phenomenon is not of relevance for the electric field effect discussed here. (Furthermore, simulations of difference decays, based on the assumption that the observed electric field effect results exclusively from a change of the rate constant for non-radiative decays, are not in agreement with the experimentally determined difference decays – results not shown).

For the evaluation of difference decays, in contrast to the data evaluation leading to the rate constants shown in Fig. 5, it was not necessary to correct the data for the PS I contribution to the fluorescence decays. Also, a minor PS II subpopulation, insensitive to electric fields, should not affect the conclusion stated above. In this event the conclusion would refer only to the field-sensitive fraction.

Determination of PS II charge separation rate constants

Our approach to correct for the PS I contribution and to calculate the rate constants from the corrected initial slope, mean lifetime and the second moment has not been used previously. Therefore, we will discuss this method in more detail. A related approach, the so called 'method of moments', has been used for the analysis of picosecond fluorescence decays of non-photosynthetic materials (for Refs. see 32, 33).

In several recent studies, rate constants of the PS II charge separation reactions were determined from time-resolved fluorescence data using the kinetic model of Schatz et al. [11]. The rate constants were either calculated from the amplitudes and time-constants of

two exponential components of preparations which were assumed to be free of any PS I [9,18,34], or the rate constants were determined by means of the so-called 'target analysis' [20,28]. The first approach is not feasible in combination with the salt-jump technique used to create the electric field. The reason is that this technique requires intact thylakoid membranes which almost inevitably do contain PS I. Also, the amount of sample needed for the combination of the flow-and-mixing technique with time-resolved fluorescence measurement and the very long measuring time required for the target analysis, as done by Roelofs et al. [20] and Lee et al. [28], are not compatible.

We measured fluorescence decays of thylakoid membranes at a single emission wavelength with $1.0 \cdot 10^4$ counts per peak channel, and we fit with three exponential components. There is general agreement that under these experimental conditions a resolution of more than three components is not reasonable [10,35–41]. Most researchers also agree that none of these components can be assigned to the fluorescence emission of PS I exclusively (reviewed in Refs. 21, 42). Thus, the exponential components obtained from curve-fitting of the measured fluorescence decays represent the fluorescence kinetics of PS I and PS II; the curve-fitting by exponentials does not permit separation of the PS I contribution of the fluorescence kinetics.

The underlying idea of the data evaluation procedure is to correct for the PS I contribution by assuming that PS I contributes to the fluorescence decay with fixed, a priori-known relative amplitude and time-constant. It is often assumed that the PS I fluorescence kinetics can be approximated by a one-exponential model with a life time of about 100 ps, which contributes to the peak amplitude of a thylakoid preparation by about 20% [20,28,29]. We used $a_{PSI} = 22\%$ and $T_{PSI} = 100$ ps or 110 ps. The influence of the chosen value of T_{PSI} is demonstrated by Table I, the influence of a 10% change of a_{PSI} (not shown) is comparable.

To do the correction we determined three parameters (initial slope, S_0; mean lifetime, T_m; second moment, M) from the fluorescence decay of the thylakoid membrane. These parameters are given by the sum of the respective parameters of PS II and PS I weighted by their respective contribution to the peak amplitude. In this manner the correction of these parameters can easily be accomplished by Eqn. B5.

The fluorescence parameters S_0, T_m and M were calculated from the exponential representation of the decays, which resulted from the curve-fitting procedure. In principle, all three parameters can be calculated from the measured decay without any curve-fitting. For three reasons we prefer to calculate these parameters from the fitted decay. First, the curve-fitting procedure delivers the iterative deconvolution. Second, the curve-fitting program takes into account the possibility of a so-called 'shift' between the measured IRF and the measured fluorescence decay (see Materials and Methods), which often is not zero. Values of T_m and M, calculated directly from the measured decay, are sensitive to a non-zero shift. And third, the initial slope, S_0, cannot be determined with reasonable accuracy directly from the (deconvoluted) decay, due to the interference of high-frequency noise components.

The corrected parameters, which are assumed to give the initial slope, mean lifetime and second moment of the PS II fluorescence, were used to calculate the charge separation rate constants of PS II using Eqns. A11, A16, A17. These equations were derived directly, i.e., without any approximations or additional assumptions, from the differential equations (Eqns. A5, A6) which describe the reversible radical pair model.

The values of the PS II charge separation rate constants

From the fluorescence decays the rate constants of primary charge separation, k_1, primary charge recombination, k_{-1}, and secondary charge separation, k_2, were determined as described above. The estimation of error ranges for the rate constant values is difficult. The reason is that the errors of the time-constants and those of the amplitudes, as determined by the exponential fits, are not independent. (Visual inspection of Fig. 3 reveals that the 'scatter' of a_1 and T_2 are correlated.) Thus, a first-order error analysis, starting with these errors, would lead to unreasonable error ranges for the calculated rate constants and free energy levels. In this work we chose a different approach. The error bars in the Figs. 5–7 were calculated from the errors of the parameters S_0, T_m and M, using error propagation (for details see Materials and Methods). In the case of k_{-1}, k_2 and $\Delta\Delta G_1$, the error ranges indicated by the error bars in the Figs. 5–7 appear to be much greater than the deviations from the straight line would suggest. This disagreement might be fortuitous. Another explanation could be that, in contrast to assumption, the errors of S_0, T_m and M were also not independent. In this case an overestimate of the resulting errors is likely. In any event, as demonstrated by Table I, the most significant source of errors is probably the uncertainties resulting from the PS I correction applied.

The zero-field values of the charge separation rate constants are given in the first column of Table I. These values deviate by less than 10% from the values determined by Roelofs et al. for PS II_α units of pea chloroplasts in the open reaction center state [20], and they are very similar to the values determined by Leibl et al. for trypsinated PS II particles [9].

The k_2 value is of reasonable magnitude, as already

discussed elsewhere [9,11,21]. The k_1 value is proportional to the (intrinsic) rate constant of primary charge separation according to Eqn. A4. To get an estimate for c_e and N of Eqn. A4 we assume that PS II particles closely resemble the PS II found in the intact thylakoid membranes. Furthermore, we assume that all chlorophyll *b* and carotenoid molecules transfer excitation energy rapidly and irreversibly to chlorophyll *a*. Based on the deconvolution of the absorbance spectrum of these particles into Gaussian components done by Jennings et al. [43] and assuming that Gaussian components with a peak wavelength smaller than or equal to 660 nm do not arise from chlorophyll *a*, we computed a value of $c_e = 1.35$ for this energy concentration factor. Using a value of $N = 140$ for the number of chlorophyll *a* molecules per reaction center [44], we eventually find for the intrinsic rate constant of primary charge separation:

$$k_1^{in} = (N/c_e) \cdot k_1 = (140/1.35) \cdot 3.1 \text{ ns}^{-1} = (3.1 \text{ ps})^{-1} \quad (9)$$

This number is in excellent agreement with the rate of radical pair formation measured in PS II reaction center preparations (about 3 ps at 277 K, see ref. 2). In consideration of the uncertainties in the values of N and c_e (e.g., numbers of chlorophyll molecules per PS II is a literature value and was not determined for the thylakoid preparation actually used in the experiments reported here), the almost perfect agreement might be fortuitous. However, the calculation of k_1^{int} demonstrates that the rate constant k_1 determined from our data is of reasonable magnitude. Using this k_1^{in} and the rate constant for the reverse reaction, k_{-1}, given in Table I, we find a zero-field free energy difference of $\Delta G = -182$ meV, calculated by Eqn. A14, between the excited state of the reaction center (P680*) and the primary radical-pair state. (This free-energy difference is different from the free-energy difference between the excited antenna state and the charge separated state, which is determined by the ratio of k_1 and k_{-1}.) If we estimate the uncertainty in N to be -30 and $+40$ and for k_{-1} to be -50% and $+100\%$ (due to the uncertainties of the PS I correction) we find an uncertainty range for ΔG_1 of 182 ± 25 meV.

Relation between thylakoid voltage and free energy difference

A thylakoid voltage leads to an electric field which interacts with the dipoles of charge separated states. Thus, a thylakoid voltage changes the free energy difference of the charge separated state [8]. Electrostatics predict that, at least at relatively low thylakoid voltages, the relation between thylakoid voltage, V, and free energy shift, $\Delta\Delta G$, is linear [8,45], i.e., $\Delta\Delta G = c_G \cdot e \cdot V$ with e denoting the electron charge and c_G a dimensionless constant. However, as already pointed out in [8], a prediction of c_G purely by means of theoretical considerations or calculations appears to be difficult. In Ref. 8 we estimated a value of 0.2 for c_G of the primary charge separation step. Fig. 6 delivers a value for c_G of 0.17, which is in reasonable agreement with our previous estimate. However, the obvious scatter in Fig. 6 and the sensitivity of the number of the PS I correction (Table I) indicates a considerable uncertainty in the experimentally determined value for c_G.

Free energy dependence of primary PS II charge separation

As shown in Fig. 7, the relation between free energy shift and the rate constant of primary charge separation, k_1, appears to be linear. The rate constant increases for an increasingly negative free energy difference by about 6% per 10 meV.

Employing semiclassical and fully quantum mechanical approaches it has been possible to predict the relations between free energy differences and the rate constants of charge transfer reactions ([24,46]; for a review see ref. 24). The theoretically derived relations were used by Vos and Van Gorkom [16] to interpret electric field effects on the PS I luminescence. Boxer and co-workers and also Moser et al. employed model calculations on the free energy dependence of charge transfer rates to analyse their experimental results on the electric field effect on the bacterial reaction center [13–15]. As demonstrated by these studies, the rate constant vs. free energy relation depends on the model employed and on the values chosen for still unknown parameters (e.g., reorganization energies). The question arises of whether the free energy dependence determined for the primary charge separation of PS II may be useful as a criterion to elucidate the validity of different theoretical concepts and to determine unknown parameters. Or is the observed linear relation over a relatively small free energy range trivial and in agreement with any model?

The electric field dependence (but not absolute value) of the rate constant of primary PS II charge transfer separation was calculated for four different theoretical models by Eqns. C1–C7. Some results are shown in Fig. 8; the calculations are briefly discussed below.

The dotted line in Fig. 8 represents the experimentally found increase of the rate constant of primary charge separation of 6% per 10 meV (Fig. 7). For all calculations a ΔG_1 value of 182 meV was used (as given in Table I).

(1) The lowest Gaussian-shaped curve was obtained for an activationless one-step electron transfer in the high-temperature limit (Eqn. C1, Refs. 24, 26). All vibrational modes which couple to the electron transfer are assumed to be so-called low frequency (lf) modes, i.e., the mode energies are smaller than kT (high-tem-

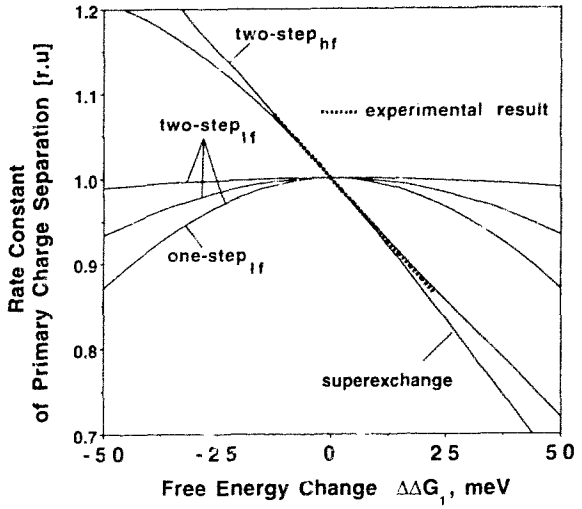

Fig. 8. Free energy dependence of the rate constant of primary charge separation, k_1, as suggested by the experimental results and by model calculations. The dotted line gives the change of k_1 by 6% per 10 meV change in free energy difference, as found in Fig. 7. The curve for the one-step electron transfer was calculated for an activationless one-step electron transfer coupled to low-frequency modes only [24,46]. Using the treatment of Bixon and Jortner [12], the line labeled 'superexchange' was obtained for a superexchange-mediated electron transfer involving a virtual intermediate with $\delta E = 165$ meV, $\nu = 0.5$ (ν and δE as defined in the text). The two-step models assume an intermediate electron acceptor between P680 and pheophytin. The lines labeled with 'two-step$_{ll}$' were obtained under the assumption of an activationless energy transfer for the first rate-limiting step coupled to low-frequency modes, with (d as defined in the text): $d = 0.2$, (top curve), $d = 0.5$ (middle curve), $d = 0.7$ (bottom curve). The 'two-step$_{hf}$' was calculated for a sequential electron transfer coupled to high-frequency nuclear modes represented by an average mode energy of 70 meV. For further details, see text.

perature limit); the reorganization energy is assumed to be equal to the zero-field free energy difference resulting in an activation energy of zero. There are no free parameters.

(2) The three Gaussian-shaped curves give the free energy difference of k_1^{in} for a (sequential) two-step model of activationless energy transfer in the high-temperature limit (Eqn. C2, C3, see Refs. 12, 24, 46) involving an hypothetical intermediate, X. Because in the isolated PS II reaction-center complex the disappearance of the excited state and the formation of a bi-radical seem to occur with approximately the same time-constant [2,22], we conclude that the first step should be rate-limiting (i.e., only this step determines the rate constant k_1^{in}). The electric field-induced free energy change of this step is given by $d \cdot \Delta\Delta G_1$. The factor d is determined by the distances between the redox centers and by the dielectric properties of the intervening medium. (To a first approximation d is given by: $d = d_{P680\text{-}X}/d_{P680\text{-}Pheo}$ with $d_{P680\text{-}X}$ and $d_{P680\text{-}Pheo}$ being projections of the respective distance vectors on the membrane normal.) The zero-field free energy difference of the rate-limiting step, $\Delta G_{1,1}$ is assumed to be -90 meV. For any combination of the free parameters d and $DG_{1,1}$, the calculated relations do not match the experimental results.

(3) The free energy dependence for the superexchange mechanism was calculated according to Bixon and Jortner [12] for a one-step electron transfer mediated by a hypothetical virtual intermediate, X. Therefore, the change of the electronic coupling was calculated according to Eqn. C5. (In (1), (2), and (4) calculations the electronic coupling is assumed to be field-independent.) A reasonable fit of the experimental relation is obtained if:

$$\delta E = \nu \cdot 330 \text{ meV} \qquad (10)$$

(δE gives the vertical energy difference between the virtual intermediate energy surface and the intersection point of the {P680*,Pheo} and the {P680$^+$,Pheo$^-$} energy surface, see ref. 12; the field-induced changes of δE are given by $\Delta\delta E = \nu \cdot \Delta\Delta G_1$, where ν is a dimensionless constant.)

(4) The free energy dependence was calculated for a two-step mechanism with coupling to high-frequency nuclear modes with an average mode energy of 70 meV (according to Eqn. C7). It has been shown by Moser et al. [26] that the free energy dependence of a variety of biological electron-transfer reactions is in agreement with this concept. For $d = 0.5$ and $\Delta G_{1,1} = -90$ meV (d and $\Delta G_{1,1}$ defined as in (2)) a fit of the experimental data is obtained with a reorganization energy of 370 meV. For d values smaller than 0.3, with reasonable parameter sets, no fit is possible.

For the calculations (1)–(3) it was assumed that the activation energy for the charge-separation reaction is zero. The assumption of activationless energy transfer is based on the finding that, for the isolated PS II reaction center complex, no decrease of the rate constant of primary charge separation accompanies a decrease in temperature from 277 K to 15 K [2,22]. It is often assumed that the activationless character of biological electron transfer reactions results from an evolutionary optimization of the rate of electron transfer. There is no proof that the primary electron transfer is still activationless in the case of the PS II complex which is embedded in the thylakoid membrane. However, the identity of k_1^{in} determined in this study and of the rate constant measured for the primary charge separation of the isolated complex supports the conclusion that the membrane environment does not add an activation energy which leads to a decreased rate constant. Furthermore, the optimization argument would not be reasonable, if it held for isolated reaction center complexes but not for electron transfer in the in vivo environment.

We compared four different theoretical concepts for the primary charge separation with our experimental results. This comparison does not lead to a simple conclusion as to which mechanism of the primary PS II charge separation is the 'real' one. Obviously, the treatments involving a one-step or two-step activationless electron transfer in the high temperature limit are not in agreement with our experimental results. Model 3 or model 4 may be appropriate; however, a more conclusive test of these concepts requires knowledge of free parameters (Model 3: ν, $\Delta G_{1,1}$, δE; Model 4: d, $\Delta G_{1,1}$, λ) or/and a much more extended range of free energy changes. Furthermore, more complex theoretical models may be required to get an adequate description of the kinetics of photosynthetic charge-separation reactions. In any event, the comparison with model calculations shown in Fig. 8 demonstrates that the observed linear free energy dependence is not trivial. A comparison of the experimentally determined free energy dependence of the rate constant of primary charge separation with model calculations appears to be a potentially useful tool to elucidate the validity of different concepts of primary charge separation.

The observed free energy dependence cannot be compared directly with results from electric field studies on the primary charge separation of photosynthetic bacteria [14,47–49]. The reason is that different approaches were used to create the electric field, which, for the experiments on bacteria, results in multiple orientations of the electric field relative to the charge transfer reaction. Nevertheless, some features can be compared. The free energy dependence of the rate constant of primary charge separation which Lockhart et al. proposed, based on results on isotropic samples (Fig. 9 in Ref. 14), is characterized by an approximately linear relation for free energy levels close to the zero-field value with a slope of about 2.5% per 10 meV. Also, the data of Popovic [49] are suggestive of a linear relation between primary charge separation and free energy difference for free energy levels close to the zero-field value. According to the analysis given in Ref. 13, the best fit of the data is obtained by assuming a superexchange model with a δE value close to the value predicted by Eqn. 10. In conclusion, not only the values for the rate constants of primary charge separation, but also their free energy dependence seem to indicate a remarkable kinetic similarity between the primary charge separation in the reaction centers of purple bacteria and in those of PS II of higher plants.

Free energy dependence of the quinone reduction

For three reasons, the data presented here do not allow us to make a clear statement about the free energy dependence of the rate constant of secondary charge separation. First, we do not know the factors which mediate between the thylakoid voltage and the free energy shift for the quinone-chlorophyll biradical. second, the scatter for the k_2 value in Fig. 5 is fairly large. Third, most likely k_2 represents mainly the secondary charge separation, i.e., quinone reduction, but to some extent also the decay of the primary bi-radical by other pathways (radiationless recombination, triplet decays). The only possible statement is that the dependence of k_2 on the thylakoid voltage is not very pronounced. We estimate that k_2 changes by less than 15% within the accessible range of thylakoid voltages.

Mechanism of the variable PS II fluorescence

Upon reduction of the primary quinone acceptor, Q_a, the fluorescence yield of PS II increases by a factor of 2 to 5 [50]. The origin of this variable fluorescence has been a matter of discussion since its discovery. Initially Q_a was assumed to be the primary acceptor. Therefore, the decay of fluorescent antenna states by initiation of the electron transfer reaction to Q_a was assumed to be blocked upon Q_a reduction. However, the discovery of pheophytin acting as the primary electron acceptor [51–54] and the observation that the variable fluorescence results from reduction of Q_a in the presence of the unreduced pheophytin, invalidated this simple explanation for the origin of the variable fluorescence. Then, Klimov proposed that, in the presence of the reduced quinone acceptor, the primary electron transfer reaction is initiated; however, this initial charge separation is followed by the recombination of the primary biradical leading to an excited state of the electron donor [53]. The decay by fluorescence of this re-excited state of the chlorophyll donor was assumed to be the origin of the variable fluorescence. The pure version of this elegant hypothesis, however, cannot be reconciled with more recent time-resolved fluorescence studies [17]. Schatz et al. [11] extended the Klimov model by formulating the reversible radical pair model described in the Appendix A. According to this model the variable fluorescence results partially from an increased recombination rate upon Q_a reduction as proposed by Klimov. However, the main reason for the fluorescence increase is considered to be a decrease in the rate of primary charge separation upon Q_a reduction which arises from a still unknown mechanism. Schatz et al. suggested that this decrease results from an electric field which is the consequence of the reduced quinone. There can be no doubt that the quinone reduction leads to local electric fields. Our study now demonstrates that electric fields indeed affect the rate constant of primary charge separation, thus providing experimental evidence in favor of the hypothesis of Schatz et al. [11].

According to Leibl et al. [9] the rate constants of primary charge separation and primary charge recombination change upon Q_a reduction; according to Schatz et al. [11,18] the recombination rate constant remains

unaffected. The reason for this discrepancy is not known. Our results indicate that both reactions (primary charge separation and primary charge recombination) are electric-field dependent. This finding seems to be more in line with the results of Leibl et al. [9]. However, the local electric field, which may lead to the increase in the fluorescence emission upon trap-closure, is likely to be much larger than the external electric fields used in this study. Therefore, it cannot be excluded that at a certain field strength the value for the charge recombination rate constant is very similar to its zero-field value.

Influence of PS II heterogeneities

In the interpretation of our electric field data we did not consider the possibility that different populations of PS II may be characterized by a different set of rate constants and that they might exhibit a different sensitivity to electric fields.

Roelofs et al. were assuming that the time-resolved fluorescence data are best described by assuming two different PS II populations. In the F_0-state, i.e., with oxidized quinone acceptor, these populations were characterized by nearly the same rate constant values for k_1, k_{-1} and k_2; under F_m conditions the rate constant sets of the two populations were found to be different. These results are a hint that there may exist a heterogeneity in the primary and secondary charge separation reactions. At the moment it is not clear to what extent possible PS II heterogeneities influence our conclusions; further studies on this question are required.

Acknowledgements

This research was supported by the Director, Office of Energy Research, Office of Basic Energy Sciences, Energy Biosciences Division of the U.S. Dept. of Energy under contract DE-AC03-76F00098. We gratefully acknowledge the support of the Alexander von Humboldt-Stiftung in form of a Feodor Lynen Fellowship (to H.D.). H.D. wants to thank Yvonne Gindt for the excellent training on the laser system and Karen White for her skillful help in sample preparation.

Appendix A

The reversible radical pair model

According to the reversible radical-pair model, excitation energy transfer between different antenna pigments and between antenna pigments and the reaction center (P680) chlorophyll(s) is fast, and so-called exciton equilibration is obtained within about 20 ps. Exciton equilibration means that the probability for the excited state to reside on a certain pigment is approximately proportional to the Boltzman factor $e^{-hc/(\lambda kT)}$ with λ giving the wavelength at the absorption peak of the pigment. (For a more detailed theoretical analysis of the excitation equilibration approximation see refs. 55, 56.) Thus, after exciton equilibration has taken place, the probability for the excited state to reside on the reaction center, p_{rc}, is given by (N_i = number of pigments with absorption peak at λ_i; λ_{rc} = 680 nm);

$$p_{rc} = c_e(1/N) \tag{A1}$$

with

$$N = \text{number of antenna pigments} = \sum N_i \tag{A2}$$

c_e = energetic concentration factor

$$= e^{hc/(\lambda_{rc}kT)} / \left\{\sum (N_i/N) \cdot e^{hc/(\lambda_i kT)}\right\} \tag{A3}$$

(The assumption of rapid exciton equilibration is definitely not valid at low temperatures, nor for phycobilisome-containing PS II complexes of cyanobacteria.) After exciton equilibration, the effective rate constant of excited state decay by primary charge separation, k_1, is given by the product of the probability to find the excited state at the reaction center, p_{rc}, times the (intrinsic) rate constant for the electron transfer from P680 to the pheophytin.

$$k_1 = p_{rc} \cdot k_1^{in} = c_e \cdot (1/N) \cdot k_1^{in} \tag{A4}$$

For $c_e = 1$, Eqn. A4 corresponds to the Pearlstein equation for the trap-limited case (Eqn. 14 in Ref. 57). Excited antenna states may also decay by radiative decays, k_F, and nonradiative decays, k_{nr}, these two decay paths are summarized under the rate constant k_A. The primary biradical state {P680$^+$,Pheo$^-$} is formed by the primary charge separation. The decay of this state by recombination to the excited singlet state of the reaction center (reformation of P680*) is described by the rate constant k_{-1}. Also, the state {P680$^+$,Pheo$^-$} may decay by means of electron transfer to the primary quinone or by triplet formation. These decay paths are summarized under the rate constant k_2. Thus, the kinetics of excited antenna states (state A) and the primary biradical (state B) after delta-pulse excitation are described by the following differential equations:

$$dA/dt = -(k_1 + k_A) \cdot A + k_{-1} \cdot B, \quad A(t=0) = A_0 \tag{A5}$$

$$dB/dt = -(k_{-1} + k_2) \cdot B + k_1 \cdot A, \quad B(t=0) = 0 \tag{A6}$$

By solving these differential equations, a bi-exponential decay of the excited antenna state A, is found; the fluorescence emission $F(t)$ is given by $k_F \cdot A(t)$. The amplitude ratio and both time-constants are relatively complicated functions of all rate constants. They can be found in Refs. 9, 11.

For the fluorescence yield, y, and the mean lifetime, T_m, of the fluorescence decay we obtain:

$$y = k_f/(k_A + (1-r)k_1) \quad (A7)$$

$$T_m = 1/(k_A + (1-r)k_1) \quad (A8)$$

with the reversibility factor, r, is given by:

$$r = k_{-1}/(k_{-1} + k_2) \quad (A9)$$

Small changes of the fluorescence yield which originate from changes of k_1, k_{-1} or k_2 are approximately given by (for $k_A \ll k_1$):

$$\Delta y/y = -\Delta k_1/k_1 + r\cdot\Delta k_{-1}/k_{-1} - r\cdot\Delta k_2/k_2 \quad (A10)$$

From the initial slope S_0, the mean lifetime T_m and the second moment M of the resulting fluorescence decay (Eqns. 4–6) the following parameters can be calculated if a value for k_A is assumed. (In this work we assume that $k_A = 0.3\ ns^{-1}$; however, the k_A value is uncritical as long as $k_A \ll S_0$, see also Table I.)

$$k_1 = S_0 - k_A \quad (A11)$$

$$r = k_{-1}/(k_{-1} + k_2) = (S_0 - 1/T_m)/k_1 \quad (A12)$$

$$g_1 = k_1/k_{-1} = (M/T_m^2 - 1)/r^2 \quad (A13)$$

$$\Delta G_1 = -kT\cdot\ln(k_1^{in}/k_{-1}) = -kT\cdot\ln(g_1) + kT\cdot\ln(c_c/N) \quad (A14)$$

$$\Delta\Delta G_1 = kT\cdot\{\ln(g_1) - \ln(g_1')\} \quad (A15)$$

$$k_{-1} = k_1/g_1 \quad (A16)$$

$$k_2 = (1/r - 1)k_{-1} \quad (A17)$$

Appendix B

PS I correction

The initial decay rate $R_{init} = dF/dt$ is the sum of the initial decay rates of PS II and PS I.

$$R_{init} = R_{init,PSI} + R_{init,PSII} \quad (B1)$$

The initial slope, S_0, of the fluorescence decay is given by the initial decay rate divided by the peak amplitude. Hence:

$$S_0 = R_{init}/A \quad \text{with} \quad A = A_{PSI} + A_{PSII} \quad (B2)$$

$$S_0 = k_{init,PSI}/A + k_{init,PSII}/A = (A_{PSI}\cdot S_{PSI})\cdot A + (A_{PSII}\cdot S_{PSII})/A \quad (B3)$$

$$S_{PSII} = (A/A_{PSII})\cdot\{S_0 - (A_{PSI}/A)\cdot S_{PSI}\} \quad (B4)$$

The same consideration holds for the mean lifetime, T_m, and the second moment, M. Thus:

$$X_{PSII} = (A/A_{PSII})\cdot\{X - (A_{PSI}/A)\cdot X_{PSI}\} \quad \text{with} \quad X = S_0, T_m, M \quad (B5)$$

Appendix C

Electric field dependence of the primary charge separation

The ratio between two electron transfer rates was calculated according to Fermi's Golden Rule:

$$k_{et}'/k_{et}^0 = (V_{et}'/V_{et}^0)^2(FC_{et}'/FC_{et}^0) \quad (C1)$$

with V', V^0 matrix elements of electronic coupling; FC', FC^0, Frank-Condon factors.

Four models, which differ in respect to the electric-field dependence of either the electronic coupling or the Frank-Condon factors, were considered. In all calculations, a value of 26 meV was used for kT; ΔG_1 gives the zero-field free energy difference for the electron transfer from the donor P680 to the acceptor pheophytin, $\Delta\Delta G_1$ gives the electric field induced change of this free energy difference.

(1) One-step activationless electron transfer in the high temperature limit (see Refs. 24, 46, the reorganization energy is assumed to be equal to the free energy difference).

$$V'/V^0 = 1, \quad FC'/FC^0 = \exp\{-\Delta\Delta G_1^2/(4\Delta G_1 kT)\} \quad (C1)$$

(2) Two-step activationless electron transfer in the high-temperature limit with the first step being rate-limiting (see Refs. 12, 24, 46, the reorganization energy of the first step is assumed to be equal to its free energy difference).

$$k_{et}'/k_{et}^0 = k_{1,1}'/k_{1,1}^0 \quad (C2)$$

$$V_{1,1}'/V_{1,1}^0 = 1, \quad FC_{1,1}'/FC_{1,1}^0 = \exp\{-(d\cdot\Delta\Delta G_1)^2/(4\Delta G_{1,1}kT)\} \quad (C3)$$

with the subscript '1,1' referring to the first electron transfer reaction. The factor d is defined as:

$$d = \Delta\Delta G_{1,1}/\Delta\Delta G_1 \quad (C4)$$

(3) Superexchange mechanism treated as a one-step activationless electron transfer in the high-temperature limit mediated by a virtual intermediate (see refs. 12, 14).

$$V'/V^0 = \delta E/(\delta E + r\cdot\Delta\Delta G_1).$$

$$FC_1'/FC_1^0 = \exp\{-\Delta\Delta G_1^2/(4\Delta G_1 kT)\} \quad (C5)$$

$$\text{with:} \quad r = \Delta\delta E/\Delta\Delta G_1 \quad (C6)$$

δE gives the vertical energy difference between the virtual intermediate energy surface and the intersection point of the {P680*,Pheo} and the {P680$^+$,Pheo$^-$} energy surface.

(4) Two-step electron transfer with coupling to high-frequency modes with an average mode energy of 70 meV (see Ref. 26).

$$V'_{1,1}/V''_{1,1} = 1, \quad FC'_{1,1}/FC''_{1,1} = I_{p'}(\lambda/125\ \text{meV})/I_{p_0}(\lambda/125\ \text{meV}) \tag{C7}$$

with $p' = -(\Delta G_{1,1} + d \cdot \Delta\Delta G_1)/70$ meV, $p_0 = -\Delta G_{1,1}/70$ meV, λ the reorganisation energy, d given by Eqn. C4 and $I_p\{\ \}$ denoting modified Bessel functions of order p.

References

1 Van Mieghem, F.J.E., Satoh, K. and Rutherford, A.W. (1991) Biochim. Biophys. Acta 1058, 379–385.
2 Wasielewski, M.R., Johnson, D.G., Seibert, M. and Govindjee (1989) Proc. Natl. Acad. Sci. USA 86, 524–528.
3 Diner, B. and Joliot, P. (1976) Biochim. Biophys. Acta 423, 479–498.
4 Joliot, P. and Joliot, A. (1974) in Proceedings of the Third International Congress on Photosynthesis (Avron, M., ed.), pp. 25–39, Elsevier, Amsterdam.
5 Meiburg, R.F. Van Gorkom, H.J. and Van Dorssen, R.J. (1983) Biochim. Biophys. Acta 724, 352–358.
6 Bulychev, A.A., Niyazova, M.M. and Turovetsky, V.B. (1986) Biochim. Biophys. Acta 850, 218–225.
7 Dau, H., Windecker, R. and Hansen, U.-P. (1991) Biochim. Biophys. Acta 1057, 337–345.
8 Dau, H. and Sauer, K. (1991) Biochim. Biophys. Acta 1098, 49–60.
9 Leibl, W., Breton, J., Deprez, J. and Trissl, H.-W. (1989) Photosynth. Res. 22, 257–275.
10 Keuper, H.J.K. and Sauer, K. (1989) Photosynth. Res. 20, 85–103.
11 Schatz, G.H., Brock, H. and Holzwarth, A.R. (1988) Biophys. J. 54, 397–405.
12 Bixon, M. and Jortner, J. (1988) J. Phys. Chem. 92, 7148–7156.
13 Moser, C.C., Alegria, G., Gunner, M.R. and Dutton, P.L. (1988) Israel J. of Chem. 28, 133–139.
14 Lockhart, D.J., Kirmaier, C., Holten, D. and Boxer, S.G. (1990) J. Phys. Chem. 94, 6987–6995.
15 Franzen, S., Goldstein, R.F. and Boxer, S.G. (1990) J. Phys. Chem. 94, 5135–5149.
16 Vos, M.H. and Van Gorkom, H.J. (1990) Biophys. J. 58, 1547–1555.
17 Schatz, G.H. and Holzwarth, A.R. (1986) Photosynth. Res. 10, 309–318.
18 Schatz, G.H., Brock, H. and Holzwarth, A.R. (1987) Proc. Natl. Acad. Sci. USA 84, 8414–8418.
19 Roelofs, T. and Holzwarth, A.R. (1990) Biophys. J. 57, 1141–1153.
20 Roelofs, T.A., Lee, C.-H. and Holzwarth, A.R. (1992) Biophys. J. (in press).
21 Holzwarth, A.R. (1991) in The Chlorophylls (Scheer, H., ed.), pp. 1125–1151, CRC Press, Boca Raton.
22 Wasielewski, M.R., Johnson, D.G., Govindjee, Preston, C. and Seibert, M. (1989) Photosynth. Res. 26, 89–99.
23 Michel, H. and Deisenhofer, J. (1988) Biochemistry 27, 1–7.
24 Marcus, R.A. and Sutin, N. (1985) Biochim. Biophys. Acta 811, 265–322.
25 Moser, C.C., Keske, J.M., Warncke, K. and Dutton, P.L. (1991) Biophys. J. 59, 521a.
26 Moser, C.C., Keske, J.M., Warncke, K., Farid, R.S. and Dutton, P.L. (1992) Nature 355, 796–802.
27 Haehnel, W., Nairn, J.A., Reisberg, P. and Sauer, K. (1982) Biochim. Biophys. Acta 680, 161–173.
28 Lee, C.-H., Roelofs, T.A. and Holzwarth, A.R. (1990) in Current Research in Photosynthesis (Baltscheffsky, M., ed.), Vol. 1, pp. 387–390, Kluwer Academic Publishers, Dordrecht.
29 McCauley, S.W., Bittersmann, E., Mueller, M. and Holzwarth, A.R. (1990) in Current Research in Photosynthesis (Baltscheffsky, M., ed.), Vol. II, pp. 297–300, Kluwer Academic Publishers, Dordrecht.
30 Briantais, J.M., Vernotte, C., Krause, G. and Weis, E. (1986) in Light Emission by Plant and Bacteria (Govindjee, Amesz, J. and Fork, D.C., eds.), pp. 539–583, Academic Press, Orlando.
31 Gottfried, D.S., Stocker, J.W. and Boxer, S.G. (1991) Biochim. Biophys. Acta 1059, 63–75.
32 Libertini, L.J. and Small, E.W. (1989) Biophys. Chem. 34, 269–282.
33 O'Connor, D.V., Ware, W.R. and Andre, J.C. (1979) J. Phys. Chem. 83, 1333–1343.
34 Sparrow, R., Evans, E.H., Brown, R.G. and Shaw, D. (1989) J. Photochem. Photobiol. B3, 65–79.
35 Nairn, J.A., Haehnel, W., Reisberg, P. and Sauer, K. (1982) Biochim. Biophys. Acta 682, 420–429.
36 Karukstis, K.K. and Sauer, K. (1983) Biochim. Biophys. Acta 725, 384–393.
37 Karukstis, K.K. and Sauer, K. (1983) Biochim. Biophys. Acta 725, 246–253.
38 Haworth, P., Karukstis, K.K. and Sauer, K. (1983) Biochim. Biophys. Acta 725, 261–271.
39 Berens, S.J., Steele, J., Butler, W.L. and Magde, D. (1985) Photochem. Photobiol. 42, 51–57.
40 Karukstis, K.K. and Sauer, K. (1984) Biochim. Biophys. Acta 766, 148–155.
41 Karukstis, K.K. and Sauer, K. (1985) Biochim. Biophys. Acta 806, 374–388.
42 Geacintov, N. and Breton, J. (1987) CRC Crit. Rev. Plant Sci. 5, 1–44.
43 Jennings, R.C., Zucchelli, G. and Garlaschi, F.M. (1990) Biochim. Biophys. Acta 1016, 259–265.
44 Lam, E., Baltimore, B., Ortiz, W., Chollar, S., Melis, A. and Malkin, R. (1983) Biochim. Biophys. Acta 724, 201–211.
45 Zheng, C., Malcolm, E.D. and McCammon, J.A. (1990) Chem. Phys. Lett. 173, 246–252.
46 Jortner, J. (1976) J. Chem. Phys. 64, 4860–4867.
47 Lockhart, D.J., Goldstein, R.F. and Boxer, S.G. (1988) J. Chem. Phys. 89, 1408–1415.
48 Lockhart, D.J. and Boxer, S.G. (1988) Chem. Phys. Lett. 144, 243–250.
49 Popovic, Z.D., Kovacs, G.J., Vincett, P.S., Alegria, G. and Dutton, P.L. (1986) Biochim. Biophys. Acta 851, 38–48.
50 Duysens, L.M.N. and Sweers, H.E. (1963) in Microalgae and Photosynthetic Bacteria (Jpn. Soc. Plant Physiol., eds.), pp. 353–372, Univ. of Tokyo Press, Tokyo.
51 Klimov, V.V. and Krasnovskii, A.A. (1981) Photosynthetica 15, 592–609.
52 Klimov, V.V., Dolan, E. and Ke, B. (1981) Biophysics 26, 816–822.
53 Klimov, V.V. and Krashnowskii, A.A. (1982) Biophysics 27, 186–198.
54 Ganago, I.B., Klimov, V.V., Ganago, A.O., Shuvalov, V.A. and Erokhin, Y.E. (1982) FEBS Lett. 140, 127–130.
55 Källebring, B. and Hansson, Ö. (1991) Chem. Phys. 149, 361–372.
56 Beauregard, M., Martin, I. and Holzwarth, A.R. (1991) Biochim. Biophys. Acta 1060, 271–283.
57 Pearlstein, R.M. (1982) Photochem. Photobiol. 35, 835–844.